

A Stochastic Analysis of the Impact of Small-Scale Fluctuations on the Tropospheric Temperature Response to CO₂ Doubling

RITA SEIFFERT* AND JIN-SONG VON STORCH

Max Planck Institute for Meteorology, Hamburg, Germany

(Manuscript received 20 January 2009, in final form 7 September 2009)

ABSTRACT

The climate response to increased CO₂ concentration is generally studied using climate models that have finite spatial and temporal resolutions. Different parameterizations of the effect of unresolved processes can result in different representations of small-scale fluctuations in the climate model. The representation of small-scale fluctuations can, on the other hand, affect the modeled climate response. In this study the mechanisms by which enhanced small-scale fluctuations alter the climate response to CO₂ doubling are investigated. Climate experiments with preindustrial and doubled CO₂ concentrations obtained from a comprehensive climate model [ECHAM5/Max Planck Institute Ocean Model (MPI-OM)] are analyzed both with and without enhanced small-scale fluctuations. By applying a stochastic model to the experimental results, two different mechanisms are found. First, the small-scale fluctuations can change the statistical behavior of the global mean temperature as measured by its statistical damping. The statistical damping acts as a restoring force that determines, according to the fluctuation–dissipation theory, the amplitude of the climate response to a change in external forcing (here, CO₂ doubling). Second, the small-scale fluctuations can affect processes that occur only in response to the CO₂ increase, thereby altering the change of the effective forcing on the global mean temperature.

1. Introduction

Determining the climate response to increasing CO₂ concentration with the aid of climate models involves several uncertainties. The estimates for the equilibrium climate sensitivity vary from model to model. The equilibrium climate sensitivity is generally defined as the equilibrium change in global surface temperature resulting from a doubling of CO₂ concentration. The main reason for the different climate sensitivities simulated by the different models is the imperfect representation of processes related to thermodynamical feedbacks, for example, cloud feedbacks, water vapor feedback, and surface albedo feedbacks (Colman 2003; Soden and Held 2006; Webb et al. 2006; Bony et al. 2006).

* Current affiliation: Federal Waterways Engineering and Research Institute, Department of Hydraulic Engineering in Coastal Areas, Hamburg, Germany.

Corresponding author address: Rita Seiffert, Wedeler Landstr. 157, Federal Waterways Engineering and Research Institute, Department of Hydraulic Engineering in Coastal Areas, Hamburg, D-22559 Germany.
E-mail: rita.seiffert@baw.de

However, other factors also affect the modeled climate sensitivity. In a previous study (Seiffert and von Storch 2008, hereafter SS08), we showed that the presence of enhanced small-scale fluctuations can affect the model's sensitivity to a doubling of CO₂ concentration. Using the comprehensive climate model ECHAM5/MPI-OM developed at the Max Planck Institute for Meteorology, we carried out equilibrium climate change experiments with enhanced small-scale fluctuations. To enhance small-scale fluctuations we either reduced the horizontal diffusion or added white noise to spectral coefficients with high total wavenumbers. In SS08, we found that the largest effects of the enhanced small-scale fluctuations on the temperature response occur in the upper troposphere at about 300 hPa. There, the equilibrium temperature response is increased by up to 14% in experiments with reduced horizontal diffusion and decreased by up to 36% in experiments with additional noise.

In SS08, however, it remains unclear via which mechanisms small-scale fluctuations can affect the tropospheric temperature response. Because small-scale fluctuations are omnipresent and always need to be parameterized in climate models, it is important to understand how they affect the temperature response to a CO₂ doubling. To

achieve this goal, we use a stochastic model to investigate how enhanced small-scale fluctuations influence the tropospheric temperature response.

a. Fluctuation–dissipation theorem

A study by von Storch (2004) provides the main motivation for the present stochastic approach. Von Storch (2004) showed that the representation of small-scale variables is crucial for the temporal statistics of large-scale variables. Because the temporal statistics of large-scale variables are linked to the response of the system to increased CO₂ concentration via the fluctuation–dissipation theorem (FDT), the mean response can depend on the representation of small-scale variables.

That the characteristics of large-scale variables influence the system's response to external forcing is also found by Branstator and Selten (2009). They found that the structure of intrinsic modes of variability affect the structure of forced climate trends.

The FDT states that the response of a system to a small change in external forcing can be directly deduced from the statistics of the *undisturbed* system. This is possible because the recovery of the system from an artificial perturbation is assumed to have, on average, about the same temporal behavior as the recovery from a natural fluctuation. Although the climate system is in a stationary state, it is frequently driven away from its mean state because of internal instabilities. The way in which the system returns from these excursions back to the mean state is determined by the overall effect of the internal feedback and interaction processes, resulting in a restoring force. The FDT assumes that these same internal feedback and interaction processes also determine the response of the system to small, artificial impulsively forced perturbations. The system's response to impulsively forced perturbations can be used to estimate the mean response to any change in external forcing with the aid of linear response theory. Hence, by observing the naturally fluctuating system, we can draw conclusions about the response of the system to a constant increment in external forcing.

The FDT originates from statistical physics. Although the climate system does not satisfy all of the conditions required for the theorem, Leith (1975) first argued that the FDT could be used to approximate the climate response to small changes in external forcings. Less restrictive derivations of the FDT, which are better suited for the climate system, have been suggested by von Storch (2004) and Gritsun and Branstator (2007). Since Leith's paper, several studies have obtained promising results when testing the FDT in climate-like systems. Bell (1980) applied the FDT successfully to a model of the barotropic vorticity equation. Other studies (North et al. 1993; Cionni

et al. 2004; Langen and Alexeev 2005; Gritsun and Branstator 2007) tested the FDT in different versions of the Community Climate Model (CCM) developed at the National Center for Atmospheric Research (NCAR). Although these studies all test the FDT, they differ in many aspects. North et al. (1993) and Cionni et al. (2004) apply the theorem within a univariate environment dealing only with the statistics and response of the global mean temperature. In contrast, Langen and Alexeev (2005) and Gritsun and Branstator (2007) use a multivariate approach. Whereas most studies aim at estimating the climate response to changed solar forcing or increased CO₂ concentration, Gritsun and Branstator (2007) analyze the response to localized heat sources. They compare the global response patterns generated by the atmospheric general circulation model with the global response patterns estimated by the usage of the FDT.

b. Effects of small-scale fluctuations on large-scale statistics

In contrast to the above-mentioned studies, we do not test the FDT. We assume that it is applicable to the climate system and use it to assess which mechanisms lead to the change in climate sensitivity caused by enhanced small-scale fluctuations. The main objective of the present study is to investigate whether the enhanced small-scale fluctuations change the temporal statistics of the global mean tropospheric temperature in the undisturbed system (i.e., in experiments with preindustrial CO₂ concentration), and thereby cause the higher/lower climate response.

If, in our experiments, the enhanced small-scale fluctuations affected the temporal statistics of the global mean temperature, then the temperature response to increased CO₂ concentration would, according to the FDT, also be influenced. In other words, because the climate response depends on the statistical properties of the preindustrial climate, the response would be changed if the statistical properties were varied by enhanced small-scale fluctuations. Indeed, the study by von Storch (2004) indicates that stronger small-scale fluctuations can lead to different temporal statistics of large-scale variables.

In the next section we briefly describe the experiments carried out with ECHAM5/MPI-OM and introduce the stochastic model. In section 3 the main properties of the fitted stochastic model are presented. In section 4 we derive a simple form of the FDT and show how the temperature response can depend on the statistics of the undisturbed system. Furthermore, we describe how the parameters of the stochastic model are affected by a CO₂ doubling and enhanced small-scale fluctuations.

TABLE 1. Overview of the experiments carried out with ECHAM5/MPI-OM (atmosphere: T31L19, ocean: 3°).

	1 × CO ₂	2 × CO ₂
Control experiments, τ ₀ = 12 h, σ _{noise} = 0	ctrl1×	ctrl2×
Reduced horizontal diffusion, τ ₀ = 24 h	diffus1×_24	diffus2×_24
Reduced horizontal diffusion, τ ₀ = 36 h	diffus1×_36	diffus2×_36
Moderate noise, σ _{noise} = 3 × 10 ⁻² K (3 × 10 ⁻⁷ s ⁻¹)	noise1×_3	noise2×_3
High noise, σ _{noise} = 6 × 10 ⁻² K (6 × 10 ⁻⁷ s ⁻¹)	noise1×_6	noise2×_6

2. Method

a. Experiments with ECHAM5/MPI-OM

ECHAM5/MPI-OM is a comprehensive coupled atmosphere–ocean–sea ice general circulation model developed at the Max Planck Institute for Meteorology (MPI) in Hamburg (Germany). No flux adjustment is needed to maintain a realistic steady climate. For a detailed description of ECHAM5, see Roeckner et al. (2003, 2006). The latter also provides a comparison of the simulated climate to reanalysis data. Technical details about the ocean model can be found in Marsland et al. (2003). A description of the mean ocean circulation for the high-resolution version is given by Jungclaus et al. (2006). The coupled model is used (with different resolutions) for a wide range of applications (e.g., Pohlmann et al. 2006; Bengtsson et al. 2007; Solomon et al. 2007; Marotzke and Botzet 2007; Kloster et al. 2007; von Storch and Haak 2008). Here we used the low-resolution version [atmosphere: T31 (≈3.8° × 3.8°) and 19 vertical levels, ocean: ≈3° × 3° and 40 vertical levels].

For this study we analyze the same experiments as introduced in SS08. In the following we briefly describe the experiments; for a more detailed description, please see SS08. Table 1 defines and summarizes the experiments that are carried out. All of the experiments are at least 150 yr long. For the analysis we use the last 100 yr of integration.

Experiments ctrl1× and ctrl2× correspond to 1 × CO₂ and 2 × CO₂ integrations using the standard model with no changes of the representation of the small-scale fluctuations. In experiments diffus1×_24 (diffus2×_24) and diffus1×_36 (diffus2×_36), the horizontal diffusion is reduced under 1 × CO₂ (2 × CO₂) conditions. In ECHAM5 the horizontal diffusion in the form of a hyper-Laplacian is applied in spectral space on temperature, vorticity, and divergence. Generally, the rate of change

of the spectral coefficient $X_{l,m}$ caused by the horizontal diffusion is defined as

$$\left. \frac{\partial X_{l,m}}{\partial t} \right|_{\text{horizontal diffusion}} = -K_l X_{l,m}, \quad (1)$$

with

$$K_l = \frac{1}{\tau_0} \left[\frac{l(l+1)}{l_0(l_0+1)} \right]^q. \quad (2)$$

Here l denotes the total wavenumber, and l_0 marks the truncation scale of the model. The order of the hyper-Laplacian operator is $2q$. It depends on the vertical level. The order is 20 below the sixth model level, that is, below about 140 hPa. In the experiments with reduced horizontal diffusion, the damping time τ_0 , which controls the strength of the horizontal diffusion, is increased by a factor of 2 or 3 from the standard value of 12 to 24 or 36 h. The increase in τ_0 leads to a weaker damping and hence an enhancement of the variability of high wavenumber components. Because the high-order hyper-Laplacian is very scale selective, the increase in τ_0 does not directly affect components with small wavenumbers.

Furthermore, two pairs of experiments in which noise is added to the smallest resolved scales under 1 × CO₂ and 2 × CO₂ are considered: noise1×_3 and noise2×_3, and noise1×_6 and noise2×_6. At each time step white noise is added to the spectral coefficients of temperature, divergence, and vorticity, with a total wavenumber $l \geq 26$. Here “_3” and “_6” distinguishes between two noise intensities. In the experiments noise1×_3 and noise2×_3, the standard deviation of the noise σ_{noise} is 3 × 10⁻² K for temperature and 3 × 10⁻⁷ s⁻¹ for vorticity and divergence. In the noise1×_6 and noise2×_6 experiments, we use higher noise intensities: 6 × 10⁻² K for temperature and 6 × 10⁻⁷ s⁻¹ for vorticity and divergence. Note that if the unresolved scales vary on time scales much smaller than those of the resolved scales, their effect can be well approximated by white noise.

b. Stochastic model

To analyze how small-scale fluctuations influence the statistical properties of the global mean temperature at 300 hPa, we will fit a nonlinear Langevin equation

$$\dot{x}_s(t) = h(x_s) + g(x_s)\eta(t) \text{ [S]} \quad (3)$$

to the results obtained from the ECHAM5/MPI-OM experiments. We choose the temperature at 300 hPa because at this level the largest response to CO₂ doubling occurs (SS08).

In Eq. (3) x_s represents the global mean temperature at 300 hPa from which the mean diurnal and annual cycles are removed and the long-term variability associated with the interactions between the ocean and the atmosphere is filtered out. The filtering procedure is described in the appendix. The long-term variability resulting from the atmosphere–ocean interactions is filtered out, because we are interested in modeling the temporal behavior of the global mean tropospheric temperature resulting from atmospheric processes only. We expect that the enhanced small-scale fluctuations primarily influence the short-term atmospheric feedback processes (e.g., cloud feedbacks, water vapor feedback). The other variables in Eq. (3) have the following meanings: \dot{x}_s denotes the time derivative of x_s , t denotes time, $\eta(t)$ represents white noise, and $h(x_s)$ and $g(x_s)$ are deterministic functions, which need to be estimated.

Equation (3) models the time evolution of x_s in a compact way. The first term on the right-hand side represents the overall effect of the interactions between x_s and variables on similar time scales as x_s . The stochastic forcing $g(x_s)\eta(t)$ mainly comprises the interactions between x_s and processes acting on time scales much shorter than those of x_s .

The symbol [S] indicates that Eq. (3) is defined in the Stratonovich system. The distinction between Stratonovich and Itô systems is closely related to the definition of continuous white noise. While the Stratonovich definition implies a small but finite correlation between two random numbers, the Itô definition sticks to the strict mathematical definition that white noise is totally uncorrelated. For a comprehensive definition and discussion about the differences between Stratonovich and Itô calculus, see Risken (1984), Gardiner (1985), and Penland (2003). Each Stratonovich stochastic differential equation (SDE) can be transformed into an equivalent Itô SDE and vice versa. In the Itô system, Eq. (3) can be written as

$$\dot{x}_s(t) = h(x_s) + g(x_s) \frac{\partial g(x_s)}{\partial x_s} + g(x_s)\eta(t) \text{ [I]} \quad (4)$$

Where [I] stands for the Itô system. Equations (3) and (4) yield the same results if (3) is integrated in the Stratonovich sense and (4) is integrated in the Itô sense. Because Itô SDEs are easier to integrate, we will stick to the transformed Itô SDE in this study.

To determine $h(x_s)$ and $g(x_s)$, we follow the approach of Siebert et al. (1998), which is, for example, also applied by Sura (2003) and Berner (2005). Equation (4) is a stochastic differential equation, that is, a differential equation including a stochastic process. Hence, the solution of (4) contains a random term. Because for each

integration of (4) different random numbers are used, each integration represents a different trajectory in phase space. After observing a large number of trajectories we can assign each point x_s in phase space a probability $dw = \rho(x_s) dx_s$ that the infinitesimal interval $(x_s, x_s + dx_s)$ will be visited by the next trajectory. In this way a probability density function $\rho(x_s)$ can be defined. The time evolution of the probability density function of a Langevin equation is generally governed by a Fokker–Planck equation,

$$\frac{\partial \rho(x_s, t)}{\partial t} = \frac{\partial}{\partial x_s} [A(x_s)\rho(x_s, t)] + \frac{\partial^2}{\partial x_s^2} [B(x_s)\rho(x_s, t)], \quad (5)$$

where $A(x_s)$ is called the drift coefficient and $B(x_s)$ is the diffusion coefficient. [For a comprehensive introduction to statistical physics and the Fokker–Planck equation see, e.g., Gardiner (1985) and Risken (1984).]

The coefficients $A(x_s)$ and $B(x_s)$ can be directly estimated from data. The drift coefficient is equal to the local mean tendencies

$$A(x_s) = \lim_{\tau \rightarrow 0} \frac{1}{\tau} \langle x_s(t + \tau) - x_s(t) \rangle \Big|_{x_s(t)=x_s}, \quad (6)$$

and the diffusion coefficient is defined as

$$B(x_s) = \lim_{\tau \rightarrow 0} \frac{1}{2\tau} \langle [x_s(t + \tau) - x_s(t)]^2 \rangle \Big|_{x_s(t)=x_s}. \quad (7)$$

Here, $\langle \dots \rangle \Big|_{x_s(t)=x_s}$ denote conditional ensemble averages. The equilibrium climate experiments are assumed to be stationary and ergodic. Therefore, the ensemble averages can be replaced by time averages.

By knowing the Fokker–Planck equation, we can in the univariate case deduce the explicit form of the corresponding Langevin equation. In the Stratonovich system $A(x_s)$ and $B(x_s)$ are related to $h(x_s)$ and $g(x_s)$ in the following way (Risken 1984):

$$A(x_s) = h(x_s) + g(x_s) \frac{\partial g(x_s)}{\partial x_s},$$

$$B(x_s) = \frac{1}{2} [g(x_s)]^2. \quad (8)$$

Inserting the definitions of (8) into Eq. (4) yields the Itô SDE

$$\dot{x}_s(t) = A(x_s) + \sqrt{2B(x_s)}\eta(t) \text{ [I]}. \quad (9)$$

In contrast to Eq. (8), the relations between the coefficients $A(x_s)$, $B(x_s)$ and the functions $h(x_s)$, $g(x_s)$ in the Itô system would be

$$\begin{aligned} A(x_s) &= h(x_s), \\ B(x_s) &= \frac{1}{2} [g(x_s)]^2. \end{aligned} \quad (10)$$

Note that if we had defined our system in the beginning to be an Itô system we would use relations (10) and Eq. (3) marked with an [I] instead of the [S]. The resulting equation would be the same as Eq. (9). For our conclusions it makes technically no difference whether we write a [S] or an [I] next to Eq. (3). The only difference lies in the interpretation. Stating that our system is a Stratonovich system implies that $A(x_s)$ is not only determined by the deterministic drift $h(x_s)$ but also by the noise-induced drift $g(x_s)[\partial g(x_s)/\partial x_s]$. On the other hand, stating that our system is an Ito system would imply that $A(x_s)$ is determined entirely by the deterministic drift $h(x_s)$.

The method of fitting the stochastic model to the ECHAM5/MPI-OM data can be summarized as follows:

- (i) We determine x_s by subtracting the mean daily and annual cycle from the global mean temperature at 300 hPa and filtering out the long-term variability as described in the appendix.
- (ii) We estimate $A(x_s)$ and $B(x_s)$ by using their definitions (6) and (7).
- (iii) We insert $A(x_s)$ and $B(x_s)$ into (9).
- (iv) Time series of x_s can be generated by integrating (9).

Using the above-outlined method, the stochastic model (3) will be fitted to global mean temperature time series at 300 hPa for the different experiments. The differences in the fitted models will be used to assess the impact of small-scale fluctuations on climate response to CO₂ doubling.

c. Time lag τ

In practice, the implementation of point ii of the above list is not straightforward. As can be seen from (6) and (7), the definitions of the drift and diffusion coefficients involve the limit of the time lag $\tau \rightarrow 0$. When using discrete model output it is not possible to take the limit $\tau \rightarrow 0$.

The question is which time lag τ we should take for the estimation of the drift and diffusion coefficient. When fitting a stochastic model to a deterministic system it is not necessarily the best strategy to use the smallest available time step. By using a stochastic model we assume that we can treat rapid fluctuations with small correlation times as if small-scale processes behave like white noise. To be able to do this approximation we should not estimate the parameters for the Fokker-Planck equation from the smallest available time step (Berner 2005). In temperature time series obtained from deterministic climate models adjacent time steps are

highly correlated. We must take care that the time step is sufficiently large that the system can be described by a differential equation containing a white noise term.

To get an idea which time lag is sufficiently large we compute, in a similar way to Berner (2005), the decorrelation rate for different time lags. The decorrelation rate α is defined as

$$\alpha(\tau) = -\frac{1}{\tau} \ln c(\tau) \quad (11)$$

in which $c(\tau)$ denotes the autocorrelation function of the ECHAM5/MPI-OM data x_s at time lag τ . A simple Markov model following the linear Langevin equation

$$\dot{z}_1(t) = -\alpha_0 z_1(t) + \beta_0 \eta(t), \quad (12)$$

with α_0 and β_0 being constant, has, for example, the decorrelation rate $\alpha(\tau) = \alpha_0$. In this model the decorrelation rate α_0 is independent of the time lag τ . DelSole (2000) investigated a “red noise model” in which the white noise term $\eta(t)$ is replaced by random fluctuations $r_\gamma(t)$ with a small but finite decorrelation time τ_γ : $\dot{z}_2(t) = -\alpha_0 z_2(t) + \beta_0 r_\gamma(t)$. In this model the decorrelation rate increases linearly with time lags $\tau < \tau_\gamma$ and asymptotes to α_0 for $\tau > \tau_{\alpha_0} \equiv 1/\alpha_0$. For our results, this means that as long as the decorrelation rate increases linearly with time lag, we cannot assume that the deterministic small-scale fluctuations can be approximated as white noise because they are not yet decorrelated.

Figure 1a illustrates the dependency of the decorrelation rate on τ in our system. The thick gray curve represents the autocorrelation function $c(\tau)$ obtained from ECHAM5/MPI-OM data x_s . The dashed black lines are exemplary exponentially decaying correlation functions with different decorrelation rates $\alpha(\tau) = -(1/\tau) \ln c(\tau)$ for the time lags $\tau = 1 \text{ d}, 2 \text{ d}, 3 \text{ d}, \dots, 8 \text{ d}$. Especially for small time lags, there is no unique decorrelation rate that is able to reproduce the autocorrelation function $c(\tau)$ over a wider range of time lags. Because $c(\tau)$ does not decay for small time lags exponentially, the dashed lines greatly differ from each other. For larger time lags the dashed lines are more similar, implying similar decorrelation rates.

In Fig. 1b the decorrelation rate of ctrl1× against the time lag is shown. As already indicated in Fig. 1a, for small time lags the decorrelation rate strongly increases. After reaching a maximum at 5–6 days α slowly decreases again. Because of the above considerations the time lag at which the maximum occurs is chosen as the shortest time step for which the stochastic model can be fitted. A time step of 5 days is large enough to eliminate strong correlations between adjacent time steps and is

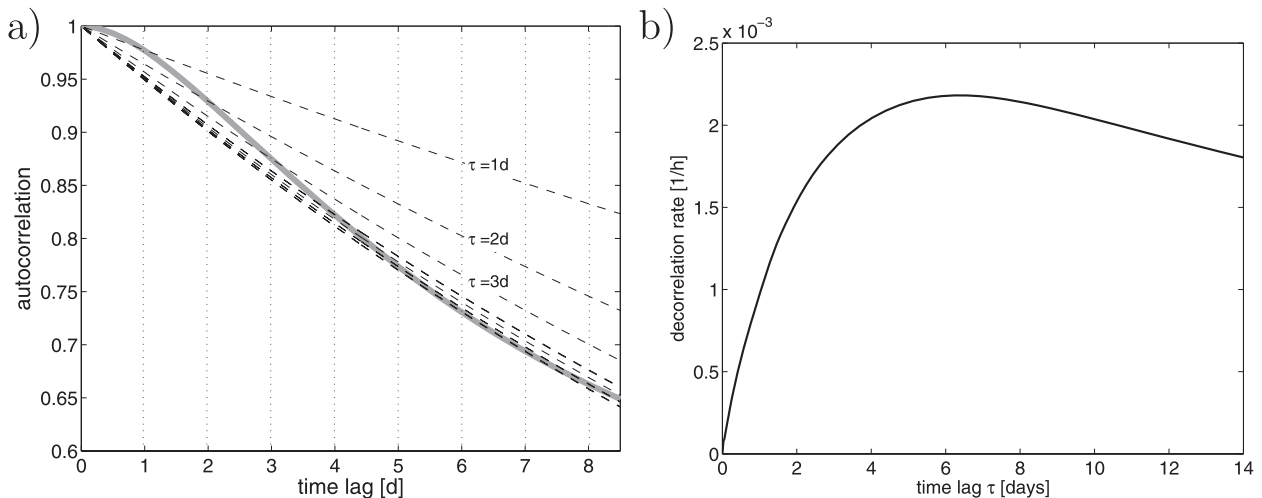


FIG. 1. (a) Autocorrelation function $c(\tau)$ of x_s obtained from experiment ctrl1 \times (thick gray line). Exponentially decaying functions fitted to match the decorrelation rate $\alpha(\tau) = -1/\tau \ln c(\tau)$ at the time lags $\tau = 1$ d, 2 d, 3 d, \dots , 8 d (dashed lines), and (b) decorrelation rate of x_s depending on the time lag τ for ctrl1 \times .

small enough to still capture the main excursions contributing to the variance of the time series.

Because the definitions (6) and (7) are only valid for the limit $\tau \rightarrow 0$, estimating the drift and diffusion coefficients by using a finite time lag leads to systematic finite-difference errors. The errors made can be estimated up to first order (Sura and Barsugli 2002), and, following Berner (2003), we could correct the coefficients. Nevertheless, in a further analysis we will use uncorrected estimates of $A(x_s)$ and $B(x_s)$, because the estimation of the error itself introduces new uncertainties and because we found that the finite-difference errors made are small (not shown).

3. Fitting the stochastic model

a. Coefficients $A(x_s)$ and $B(x_s)$

We estimate the drift coefficient $A(x_s)$ and diffusion coefficient $B(x_s)$ from data with a time lag of 5 days by dividing the phase space into 20 equidistant intervals. The main results described below do not change when we use 25, 30, or 35 intervals. Figure 2 shows the estimated coefficients $A(x_s)$ and $B(x_s)$ of the Fokker–Planck equation of the experiment ctrl1 \times . For the evaluation we used one chunk of data including 100 yr. To estimate the sampling error resulting from the usage of a finite number of data points, the gray lines represent results from 70 other chunks of data each of which are 100 yr long.

As a first approximation the drift coefficient can be characterized by a straight line, suggesting that the deterministic part of the Langevin equation represents essentially a linear damping plus a constant forcing. The diffusion coefficient is by definition everywhere positive.

In general, a constant diffusion coefficient independent of x_s would correspond to additive noise in the Langevin equation. From Fig. 2b it can be seen that $B(x_s)$ is not constant, consistent with the presence of multiplicative noise. Large temperature anomalies are on average accompanied with higher noise intensities.

b. Statistical properties

To get an impression how well the nonlinear Langevin Eq. (9) is able to reproduce main statistical properties, we compare in the following x_s , that is, the filtered global mean temperature at 300 hPa obtained from ECHAM5/MPI-OM, with data generated by integrating the stochastic model (9). The stochastic differential equation is numerically integrated by using the stochastic Euler scheme (Kloeden 1992).

Figure 3 shows the probability density function (PDF) of the ECHAM5/MPI-OM data and the PDF obtained from data generated by the stochastic model. In general, the PDF is reproduced well by the stochastic model. The PDF of the stochastic model, however, overestimates the maximum. The overestimation of the maximum is related to the too-heavy tails of the PDF of the stochastic model. The kurtosis estimated from the ECHAM5/MPI-OM data is 0.2, whereas it ranges from 0.9 to 1.5 for different realizations of the stochastic model.¹ Normally distributed data would have a kurtosis of zero.

¹ The range of 0.9–1.5 results from the calculation of the kurtosis for 40 different realizations of the stochastic model (9). Each realization has the same number of time steps as the ECHAM5/MPI-OM data; 95% of the calculated values lie within the above-given range.

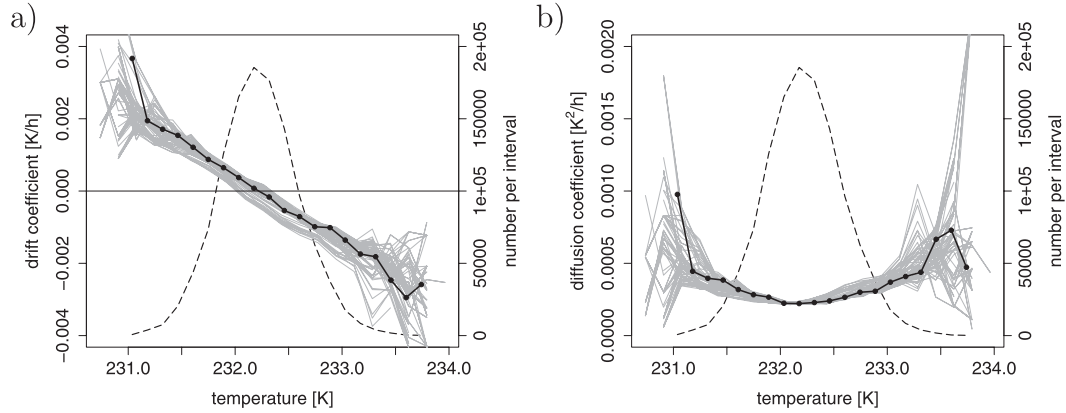


FIG. 2. Estimated coefficients of the Fokker–Planck equation for model data x_s obtained from ctrl1× (solid black lines). For the evaluation we used one chunk of data including 100 yr. Estimated coefficients from 70 other chunks each having a length of 100 yr (gray lines). The additional chunks result from an extension of the experiment ctrl1× to a total length of 800 yr as described in section 4b. Each chunk overlaps the previous chunk by 90 yr. (a) Drift coefficient $A(x_s)$ and (b) diffusion coefficient $B(x_s)$ are shown. The number of data points per interval is represented by dashed lines.

The autocorrelation function (Fig. 3b) of the stochastic model fitted to x_s resembles the autocorrelation function of the filtered ECHAM5/MPI-OM data x_s up to a time lag of $\tau \approx 20$ days well. For larger time lags the ECHAM5/MPI-OM data x_s still show some long-term variability that cannot be simulated by the stochastic model.

4. Implications of the stochastic model

a. Two ways in which the mean and its response to CO_2 doubling is affected

In Fig. 2 we noticed that the drift coefficient is approximately a linear function of temperature. Thus, we replace $A(x_s)$ in Eq. (9) with a linear function $A(x_s) = -\alpha x_s + F$, where α and F are constants. We get

$$\dot{x}_s(t) = -\alpha x_s + F + \sqrt{2B(x_s)}\eta(t) \quad [I]. \quad (13)$$

In the next steps we want to find equations for the time mean of x_s and its response to CO_2 doubling. Applying a time average to Eq. (13) yields

$$0 = -\alpha \bar{x}_s + F + 0 \quad (14)$$

Because the system is statistically stationary, the average of the time derivative $\bar{\dot{x}_s}(t)$ is zero. The vanishing of the third term on the right-hand side needs some more explanations. When integrating the Itô SDE (13) in time the next value x_s^{i+1} depends on the previous value x_s^i , $B(x_s^i)$, and a random number η^{i+1} . Because η^{i+1} is totally uncorrelated from the previous random number η^i that

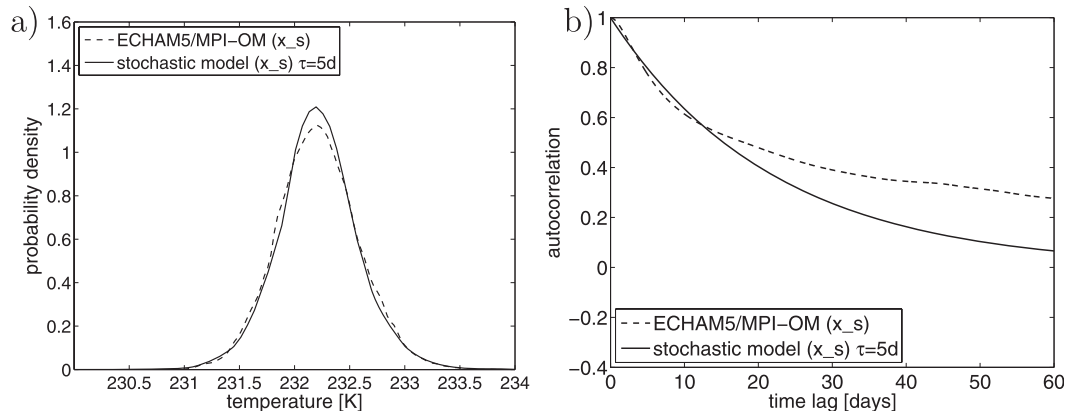


FIG. 3. (a) Probability density function of x_s extracted from ECHAM5/MPI-OM data of the experiment ctrl1× (dashed) and of the stochastic model with $\tau = 5$ d (solid); (b) autocorrelation functions of the ECHAM5/MPI-OM data x_s of ctrl1× (dashed) and of the stochastic model fitted to x_s (solid). The probability density functions were estimated by using the MATLAB-function `ksdensity`.

is used to compute x_s^i and $B(x_s^i)$, $B(x_s)$ and $\eta(t)$ are independent of each other. The time average can be applied separately on each factor of the third term on the right-hand side to yield $\frac{F}{\sqrt{2B(x_s)}\eta(t)}$. Because the mean of the noise is zero the whole term vanishes. In a Stratonovich SDE, the time mean of the term involving white noise would not be necessarily zero because $B(x_s)$ was not independent of $\eta(t)$. However, if we had derived Eq. (13) as a Stratonovich SDE, an additional term on the right-hand side would have appeared. This term should cancel the nonzero contribution from the noise term.

For the mean equilibrium state μ_1 under $1 \times \text{CO}_2$ conditions we get

$$\mu_1 \equiv \bar{x}_s = \frac{F}{\alpha}. \quad (15)$$

The mean μ_1 is solely determined by the two parameters F and α representing two distinct ways in which the mean is influenced.

The F represents the effective forcing. It results from the mean net effect of all processes within the climate system that do not depend on the actual value of x_s . For example, F includes external factors such as CO_2 concentration and solar irradiance. However, it also comprises the influence of, for example, the mean oceanic and atmospheric circulation, the mean cloud distribution, and the mean surface albedo on the global mean temperature.

The parameter α is related to the internal feedback and interaction processes that depend on the actual state of x_s . The term $-\alpha x_s$ in Eq. (13) is often referred to as statistical dissipation or damping. It is inevitable for achieving an equilibrium state under a constant forcing. The negative slope $-\alpha$ ensures the stationarity of the system and describes how the system is driven on average back toward its mean after experiencing a perturbation.

Doubling the CO_2 concentration modifies the forcing F in Eq. (13) to $F + \Delta F$. After a certain time the system reaches a new equilibrium μ_2 ,

$$\mu_2 = \frac{F + \Delta F}{\alpha}. \quad (16)$$

The response $\Delta\mu$ to the doubled- CO_2 concentration is determined by combining Eqs. (15) and (16) as

$$\Delta\mu \equiv \mu_2 - \mu_1 = \frac{\Delta F}{\alpha}. \quad (17)$$

The above relation represents a simple form of the fluctuation dissipation theorem. It is valid only if the

system can be described by Eq. (13) and the changed forcing (here the CO_2 increase) does not alter the statistical damping coefficient α . Equation (17) states that the mean response $\Delta\mu$ can be determined from knowing the statistics of the undisturbed system, namely, α , and the change in forcing ΔF .

Note that ΔF is not equal to the radiative forcing of CO_2 as considered in the Intergovernmental Panel on Climate Change (IPCC) Third and Fourth Assessment Reports. Therein, the radiative forcing of CO_2 is defined as “the change in net irradiance at the tropopause after allowing for stratospheric temperatures to readjust to radiative equilibrium but with surface and tropospheric temperatures and state held fixed at the unperturbed values” (Forster et al. 2007). In contrast, here the entire atmosphere is allowed to change. Here, ΔF represents the net change in the parameter F for 300-hPa temperature resulting from a doubling of the CO_2 concentration.

Considering relation (17), we find three possibilities of how the climate response $\Delta\mu$ can be influenced via enhanced small-scale fluctuations:

- Case 1: The numerator ΔF could be changed by the different representations of small-scale fluctuations. In other words, ΔF results not only from changes in CO_2 concentration but also from the representation of small-scale fluctuations. Because ΔF cannot be observed in the undisturbed system, the small-scale fluctuations would alter feedback and interactions processes that only occur in response to the CO_2 increase.
- Case 2: The enhanced small-scale fluctuations could lead to a larger or smaller statistical damping coefficient α . As discussed in the introduction this would mean that the statistics of the global mean temperature are altered. The small-scale fluctuations would alter feedback and interaction processes that are already present in the undisturbed system.
- Case 3: Both α and ΔF are influenced by the representation of the small-scale fluctuations. The mean temperature response is affected via both mechanisms described in cases 1 and 2.

In the following, for each experiment we estimate the drift coefficient and its slope $-\alpha$. By comparing the results we will see whether the enhanced small-scale fluctuations alter the statistics of x_s and with it the response $\Delta\mu$. We determine the drift coefficient from the last 100 yr of data of each experiment (model years 51–150 corresponding to $\approx 1\,314\,000$ time steps) by using relation (6) with $\tau = 5$ days. To get a good estimate of the slope $-\alpha$, we take the mean of three linear least squares fits differing in the number of data points used. For the fitting we use the 6, 8, or 10 midmost points, because we are interested in the slope drawn by the inner points.

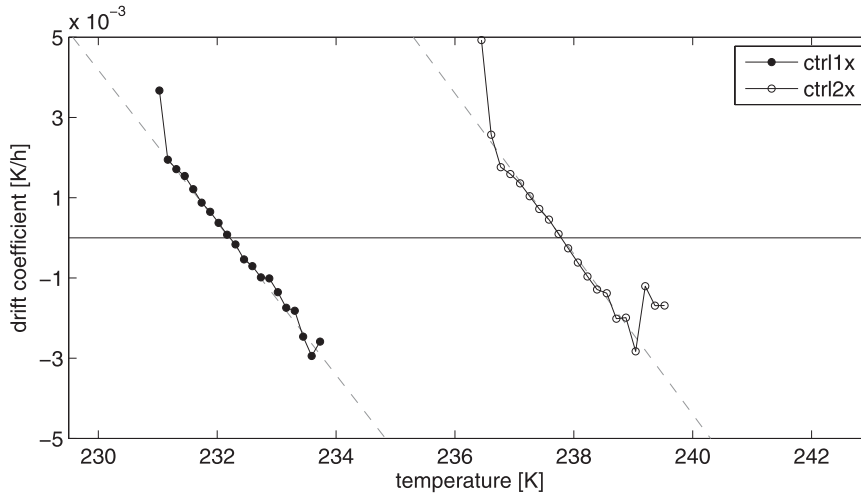


FIG. 4. Drift coefficients $A(x_s)$ of the experiments ctrl1 \times (closed circles) and ctrl2 \times (open circles) as well as a linear fit of ctrl1 \times (right gray dashed line). The linear fit of ctrl1 \times shifted along the x axis is also displayed (left gray dashed line).

b. The restoring parameter α

For the derivation of Eq. (17) we assumed that a CO₂ doubling exerts only a small change in external forcing on the system. That means the main temporal statistics, namely, the restoring mechanism ensuring the stationarity of the system, remain unchanged under $2 \times$ CO₂ conditions. Figures 4 and 5 give evidence that this assumption is justified in the climate system.

Figure 4 shows the drift coefficient $A(x_s)$ obtained from the control experiments with $1 \times$ CO₂ concentration and with $2 \times$ CO₂ concentration. The increased CO₂ concentration results mainly in a horizontal shift of the drift coefficient. The external forcing F is increased. The slope of the drift coefficient $-\alpha$ changes only little. We find $\alpha_{\text{ctrl1}\times} = 1.84 \times 10^{-3} \text{ h}^{-1}$ and $\alpha_{\text{ctrl2}\times} = 2.03 \times 10^{-3} \text{ h}^{-1}$.

To get an idea of the uncertainties involved when estimating α , we performed a nonparametric statistical test. As null hypothesis, we assume that α in experiment ctrl2 \times , $\alpha_{\text{ctrl2}\times}$, equals α in experiment ctrl1 \times , $\alpha_{\text{ctrl1}\times}$. In other words, the difference between $\alpha_{\text{ctrl1}\times}$ and $\alpha_{\text{ctrl2}\times}$ occurred just by chance. We extend the experiment ctrl1 \times by 650 yr and split the now 800-yr-long ctrl1 \times experiment into 71 chunks of data. Each chunk has a length of 100 yr and overlaps the previous chunk by 90 yr. For each chunk we estimate the statistical damping coefficient α as described above. The 71 resulting values are estimates of the parameter $\alpha_{\text{ctrl1}\times}$, which we could have obtained, if we by chance had used another chunk of 100-yr data instead of year 51–150 of the ctrl1 \times experiment.

The empirical cumulative distribution function obtained from the 71 α estimates is shown in Fig. 5. The

vertical dotted lines mark the 2.5th and 97.5th percentiles. If $\alpha_{\text{ctrl2}\times}$ were smaller than the 2.5th percentile or larger than the 97.5th percentile, we would reject the null hypothesis with 5% risk and accept the alternative hypothesis that $\alpha_{\text{ctrl2}\times}$ is statistically significantly different from $\alpha_{\text{ctrl1}\times}$. The dashed vertical line marks the estimate of $\alpha_{\text{ctrl2}\times}$. It lies within the uncertainty range of $\alpha_{\text{ctrl1}\times}$. Hence, we conclude that a higher CO₂ concentration does not significantly alter α . Our results are

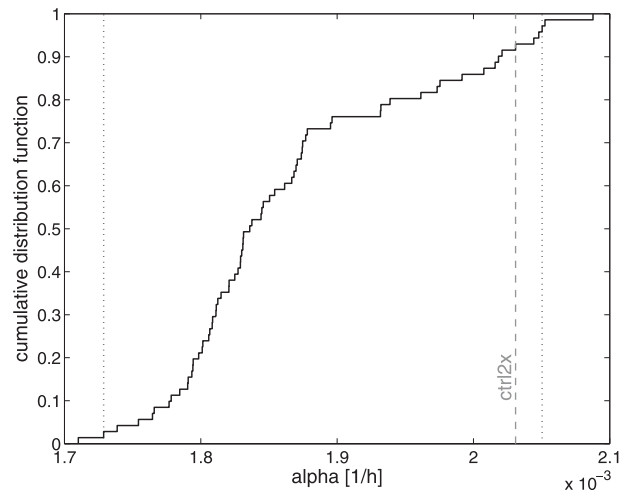


FIG. 5. Cumulative distribution function (CDF) of the parameter α obtained from the experiment ctrl1 \times . The CDF is estimated from 71 drift coefficients, which were calculated by using 71 overlapping 100-yr chunks. The 2.5th and 97.5th percentiles (dotted vertical lines) are marked, and the estimate of α for ctrl2 \times is shown (dashed vertical line).

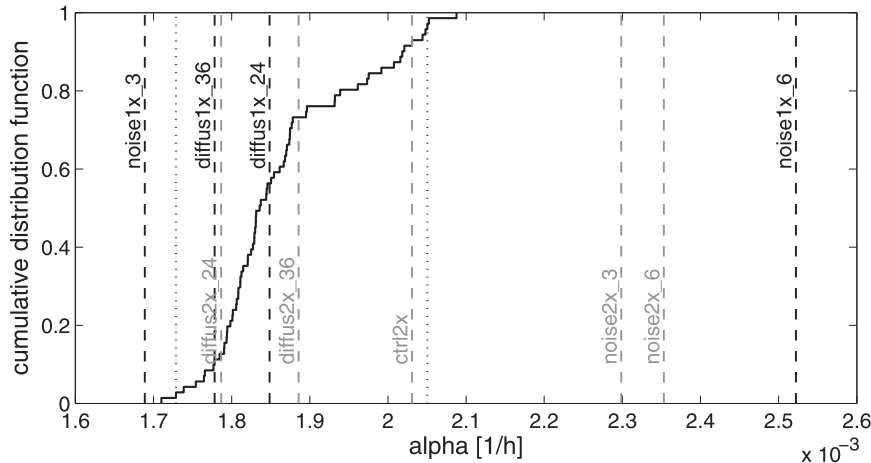


FIG. 6. CDF of the parameter α obtained from the experiment $\text{ctrl}1\times$ as shown in Fig. 5. The 2.5th and 97.5th percentiles are marked (dotted, vertical lines), and the estimates of α for different experiments as given in Table 2 are given (dashed vertical lines).

consistent with Eq. (17). The response $\Delta\mu$ is mainly due to an increase of F .

In the following we investigate whether the statistical damping coefficient α obtained from the experiments with enhanced small-scale fluctuations are significantly different from that in $\text{ctrl}1\times$. If α were changed it might be an explanation for the different temperature responses found. Figure 6 shows the α estimates of all of the experiments in the context of the cumulative distribution function estimated for $\alpha_{\text{ctrl}1\times}$; for explicit values, see also Table 2. Overall, we find distinct behaviors of the diffusion experiments and the noise experiments. Reducing the horizontal diffusion does not significantly change the statistical damping coefficient. Adding noise to the small scales, however, may result in a different statistical damping. With the exception of the experiment $\text{noise}1\times_3$ all noise experiments have a larger α . This means that the slopes of the corresponding drift coefficients are steepened. Thus, the noise strengthens the statistical damping of the global mean temperature

at 300 hPa. On average, the system with noise is driven back more strongly toward the mean state than the system without noise.

From Fig. 6 we conclude that reducing the horizontal diffusion does not change α . Because $\Delta\mu$ in the diffusion experiments is not the same as $\Delta\mu$ in the control experiments (Table 2, third column), ΔF must be different (case 1).

For the noise experiments the situation is more complicated. Because in the set of experiments with moderate noise ($\text{noise}2\times_3$ – $\text{noise}1\times_3$) α changes from the $1\times\text{CO}_2$ experiment to the $2\times\text{CO}_2$ experiment, relation (17) is not valid. The $\text{noise}1\times_3$ and $\text{noise}2\times_3$ experiments violate the assumption that a CO_2 doubling does not change the statistical damping coefficient. We cannot say whether the change in $\Delta\mu$ is caused by changes in α or ΔF .

For the set of experiments with strong noise ($\text{noise}2\times_6$ – $\text{noise}1\times_6$) cases 2 or 3 may be true, assuming that $\alpha_{\text{noise}1\times_6}$ and $\alpha_{\text{noise}2\times_6}$ are not significantly

TABLE 2. Estimates of the statistical damping coefficient α , global mean temperature response at 300 hPa to a doubling of CO_2 $\Delta\mu$, and the parameter ΔF defined in Eq. (17). The value of $\alpha_{\text{ctrl}1\times}$ corresponds to the mean obtained from the 71 α estimates used to create the cumulative distribution function in Fig. 5. Its uncertainty interval (1.73, 2.05) is based on the 2.5th and 97.5th percentiles of the cumulative distribution function. All of the other statistical damping coefficients are estimated each from a single 100-yr-long data chunk. For the sets of experiments ctrl , diffus_{24} , and diffus_{36} , ΔF is evaluated by using $\bar{\alpha}_{\text{ctrl}1\times} = 1.87 \times 10^{-3} \text{ 1/h}$ and $\Delta\mu$ of each set of experiments. For noise_6 ΔF is evaluated by using $(\alpha_{\text{noise}1\times_6} + \alpha_{\text{noise}2\times_6})/2 = 2.44$.

Set of experiments	α (10^{-3} h^{-1})		$\Delta\mu$ (K)	ΔF (10^{-3} K h^{-1})
	$1\times\text{CO}_2$	$2\times\text{CO}_2$		
Ctrl	1.87 (1.73, 2.05)	2.03	5.6	10.5
Diffus_24	1.85	1.79	6.1	11.4
Diffus_36	1.78	1.89	6.4	12.0
Noise_3	1.69	2.30	5.1	—
Noise_6	2.52	2.35	3.6	8.8

different (seeing the uncertainty range of $\text{ctrl}1\times$, this is a reasonable assumption). In comparison to the control experiments the statistical damping coefficient in experiments $\text{noise}1\times_6$ and $\text{noise}2\times_6$ changed, but we have to check whether the change of the statistical damping coefficient alone is responsible for the decrease of $\Delta\mu$ by 2 K.

c. The change in constant forcing ΔF

For the experiments in which $\alpha_{1\times\text{CO}_2} = \alpha_{2\times\text{CO}_2}$ (within the range of uncertainty), we evaluate ΔF using (17), as $\Delta F = \Delta\mu\alpha$. As a result, our estimates for ΔF are not independent measures and cannot be used for testing the validity of relation (17).

Because we found that the statistical damping coefficients in the sets of experiments ctrl , diffus_{24} , and diffus_{36} are equal within the uncertainty range, we use for the determination of ΔF of these three sets of experiments the same statistical damping coefficient $\bar{\alpha}_{\text{ctrl}1\times} = 1.87 \times 10^{-3} \text{ h}^{-1}$. Here, $\bar{\alpha}_{\text{ctrl}1\times}$ is the mean of the 71 α estimates used to create the cumulative distribution function in Fig. 5. Because the responses to CO_2 doubling are larger in the experiments, diffus_{24} and diffus_{36} compared to ctrl , and the statistical damping coefficients are taken to be equal, ΔF has to be larger in the experiments with reduced horizontal diffusion (Table 2, last column).

For the set of noise_6 experiments we evaluate ΔF by using the average of $\alpha_{\text{noise}1\times_6}$ and $\alpha_{\text{noise}2\times_6}$. We get $\Delta F_{\text{noise}_6} = 8.8 \times 10^{-3} \text{ K h}^{-1}$, which is smaller than $\Delta F_{\text{ctrl}} = 10.5 \times 10^{-3} \text{ K h}^{-1}$. Hence, we infer that in the set of noise_6 experiments the noise alters both the statistical damping coefficient α and the change in the forcing ΔF . Case 3 of the above consideration applies.

5. Discussion and conclusions

To better understand how small-scale fluctuations alter the equilibrium tropospheric temperature response to CO_2 doubling, we used a stochastic model. We fitted a nonlinear Langevin equation to global mean temperature time series at 300 hPa obtained from climate change experiments with and without enhanced small-scale fluctuations. The resulting Langevin equation has a nearly linear damping term and multiplicative noise.

a. Validity of a special form of the FDT

During this study we assumed that the fluctuation dissipation theorem (FDT) expressed in relation (17), $\Delta\mu = \Delta F/\alpha$, is applicable to our system. This special form of the FDT is only valid if we can describe the main statistical properties of the global mean temperature at 300 hPa by the Langevin equation. From Fig. 3b we see, however, that the autocorrelation function of the ECHAM5/MPI-OM

data is, especially for larger time lags, not decaying exponentially. The Langevin equation is only a crude approximation. An imperfect representation of the autocorrelation function means that Eq. (3) is not perfectly representing the time evolution of the tropospheric temperature. Despite this shortcoming we still believe that the FDT as used in this study is a useful tool for analyzing the system's response to increased CO_2 concentration and enhanced small-scale fluctuations.

Note that to truly test the validity of relation (17) we would need to obtain independent estimates of $\Delta\mu$, α , and ΔF . Whereas, we are able to determine $\Delta\mu$ and α , it is difficult to estimate ΔF . We determined ΔF by using the relation (17). Thus, ΔF is not an independent parameter; ΔF depends directly on $\Delta\mu$ and α .

b. Another condition relevant for the FDT

One important condition required for the FDT to be applicable is that the internal restoring force, as described by the correlation function or α for one-dimensional linear systems, must remain unchanged when the external forcing is perturbed. Only then can the FDT be used to determine the response to the change in the external forcing.

Obviously, such a condition will only be satisfied when the change in the forcing is sufficiently small. Does a CO_2 doubling represent such a small forcing change? Our analysis suggests that this is the case in most experiments. A CO_2 doubling leads primarily to an increase of the effective forcing F , with α remaining unchanged. The only exception is the experiment with moderate noise intensity. In this case, α is significantly changed by a CO_2 doubling. The FDT is not applicable in this case. We speculate that generally noise enhances α . However, such an impact of the noise on α is only well established when the noise is sufficiently strong. This could be the reason why we did not obtain a stable α in experiments with moderate noise.

c. Possible mechanisms responsible for changed tropospheric temperature response through enhancing small-scale fluctuations

The results of our stochastic analysis suggest that small-scale fluctuations affect the tropospheric temperature responses by altering the change in the effective forcing ΔF . Changes in ΔF resulting from enhanced small-scale fluctuations mean that ΔF depends not only on the magnitude of the CO_2 increase, but also on other factors such as the representation of small-scale processes. Here we suggest one possible chain of processes, through which different representations of small-scale fluctuations produce different values of ΔF . Table 3 shows the 300-hPa temperature and vertically integrated

TABLE 3. Mean globally averaged temperature at 300 hPa, T_{300} (K); mean globally averaged vertically integrated water vapor content q_v (kg m^{-3}); and the fractional gain of q_v , resulting from CO_2 doubling $\Delta q_v/q_v$ (where $\Delta q_v = q_v^{2\times\text{CO}_2} - q_v^{1\times\text{CO}_2}$). All numbers are based on 50-yr averages.

Experiment	T_{300}	q_v	$\Delta q_v/q_v$
Ctrl1 \times	232.2	26.0	0.32
Diffus1 \times _24	232.6	26.4	0.34
Diffus1 \times _36	232.8	26.7	0.36
Noise1 \times _3	230.8	25.8	0.30
Noise1 \times _6	230.1	24.3	0.25

water vapor in different $1 \times \text{CO}_2$ experiments. Relative to the control climate, the climates are warmer in the diffus_24 and diffus_36 experiments and colder in the noise_3 and noise_6 experiments. Because of the warmer preindustrial climates, the CO_2 doubling triggers stronger water vapor–greenhouse feedbacks in the diffusion experiments than in the control experiments. The globally averaged vertically integrated water vapor content increases, for example, in diffus_36 by 36% and in the control experiments only by 32%. The stronger water vapor–greenhouse feedback contributes to the larger change of the effective forcing ΔF . In contrast, the colder climates in the noise experiments lead to weaker water vapor–greenhouse feedbacks. The change of the effective forcing resulting from CO_2 doubling ΔF is reduced.

Changes in the statistical damping imply that the restoring force, which describes how fast the stationary system returns from a natural fluctuation to its mean, has changed. That means that the enhanced small-scale fluctuations alter the internal large-scale feedback and interaction processes. For example, negative cloud feedbacks acting in the equilibrium system could be strengthened, resulting in an overall larger negative feedback toward the mean. The system then returns faster from a natural disturbance to its mean.

d. Conclusions

We conclude that small-scale fluctuations can influence the mean temperature response to a CO_2 doubling via two different mechanisms. First, they can influence the mean temperature response via altering the statistical damping, which acts as a restoring force. That means that internal feedback and interaction processes that are present in the undisturbed system can be changed due to a different representation of small-scale processes. Second, the small-scale fluctuations can alter feedback and interaction processes that are directly coupled to the CO_2 increase. They can affect the change in forcing resulting from processes that are independent from the time-dependent state of the undisturbed system. Whereas reducing the horizontal diffusion changes the climate

sensitivity via the second mechanism, the additional noise triggers both mechanisms.

Acknowledgments. We thank Lorenzo Tomassini, Johann Jungclaus, and Klaus Hasselmann for useful discussions. We also thank two anonymous reviewers for their comments and valuable suggestions that greatly improved the manuscript. This work was supported by the Max Planck Society and the International Max Planck Research School on Earth System Modelling.

APPENDIX

Filtering Out the Long-Term Variability

In the following we describe the derivation of x_s from the global mean temperature at 300 hPa x . We assume that the time anomalies of the global mean temperature at 300 hPa, $x' = x - \bar{x}$, can be divided into two parts:

$$x' = x'_s + x'_l, \quad (\text{A1})$$

where x'_s describes the part which is associated with the internal short-term atmospheric variations and x'_l is related to the long-term variations of the atmosphere caused by the interactions of the atmosphere and the ocean. To estimate x'_l , a linear relationship between x'_l and the anomalies of the global mean sea surface temperature (SST) y' is assumed;

$$x'_l = \beta y'. \quad (\text{A2})$$

Before carrying out a least squares fit, a 90-day running mean is applied to the data. In this way we ensure that only the long-term variations contribute. Under the assumption that x'_s and $y'_{90\text{d}}$ are uncorrelated, β is estimated with

$$\beta = \frac{\langle x'_{90\text{d}} y'_{90\text{d}} \rangle}{\langle y'^2_{90\text{d}} \rangle}, \quad (\text{A3})$$

where $x'_{90\text{d}}$ and $y'_{90\text{d}}$ denote the time series on which a 90-day running mean was applied. We determine x'_s by subtracting the scaled SST anomalies from x'

$$x'_s = x' - \beta y'_{90\text{d}}. \quad (\text{A4})$$

The filtered global mean temperature at 300 hPa x_s can now be defined as

$$x_s = x'_s + \bar{x} = x - \beta y'_{90\text{d}}. \quad (\text{A5})$$

REFERENCES

- Bell, T. L., 1980: Climate sensitivity from fluctuation dissipation: Some simple model tests. *J. Atmos. Sci.*, **37**, 1700–1707.
- Bengtsson, L., K. I. Hodges, M. Esch, N. Keenlyside, L. Kornbluh, J. J. Lu, and T. Yamagata, 2007: How many tropical cyclones change in a warmer climate? *Tellus*, **59**, 539–561.
- Berner, J., 2003: Detection and stochastic modelling of nonlinear signatures in the geopotential height of an atmospheric general circulation model. Ph.D. thesis, Rheinische Friedrich-Wilhelms-Universität Bonn, 156 pp.
- , 2005: Linking nonlinearity and non-Gaussianity of planetary wave behavior by the Fokker–Planck equation. *J. Atmos. Sci.*, **62**, 2098–2117.
- Bony, S., and Coauthors, 2006: How well do we understand and evaluate climate change feedback processes? *J. Climate*, **19**, 3445–3482.
- Branstator, G., and F. Selten, 2009: “Modes of variability” and climate change. *J. Climate*, **22**, 2639–2658.
- Cionni, I., G. Visconti, and F. Sassi, 2004: Fluctuation dissipation theorem in a general circulation model. *Geophys. Res. Lett.*, **31**, L09206, doi:10.1029/2004GL019739.
- Colman, R., 2003: A comparison of climate feedbacks in general circulation models. *Climate Dyn.*, **20**, 865–873.
- DeSole, T., 2000: A fundamental limitation of Markov models. *J. Atmos. Sci.*, **57**, 2158–2168.
- Forster, P., and Coauthors, 2007: Changes in atmospheric constituents and in radiative forcing. *Climate Change 2007: The Physical Science Basis*, S. Solomon et al., Eds., Cambridge University Press, 129–234.
- Gardiner, C. W., 1985: *Handbook of Stochastic Methods: For Physics, Chemistry, and the Natural Sciences*. Springer, 442 pp.
- Gritsun, A., and G. Branstator, 2007: Climate response using a three-dimensional operator based on the fluctuation–dissipation theorem. *J. Atmos. Sci.*, **64**, 2558–2575.
- Jungclauss, J. H., and Coauthors, 2006: Ocean circulation and tropical variability in the coupled model ECHAM5/MPI-OM. *J. Climate*, **19**, 3952–3972.
- Kloeden, P., 1992: *Numerical Solution of Stochastic Differential Equations*. Springer, 632 pp.
- Kloster, S., K. D. Six, J. Feichter, E. Maier-Reimer, E. Roeckner, P. Wetzel, P. Stier, and M. Esch, 2007: Response of dimethylsulfide (DMS) in the ocean and atmosphere to global warming. *J. Geophys. Res.*, **112**, G03005, doi:10.1029/2006JG000224.
- Langen, P. L., and V. A. Alexeev, 2005: Estimating $2 \times \text{CO}_2$ warming in an aquaplanet GCM using the fluctuation–dissipation theorem. *Geophys. Res. Lett.*, **32**, L23708, doi:10.1029/2005GL024136.
- Leith, C., 1975: Climate response and fluctuation dissipation. *J. Atmos. Sci.*, **32**, 2022–2026.
- Marotzke, J., and M. Botzet, 2007: Present-day and ice-covered equilibrium states in a comprehensive climate model. *Geophys. Res. Lett.*, **34**, L16704, doi:10.1029/2006GL028880.
- Marsland, S. J., H. Haak, J. H. Jungclauss, M. Latif, and F. Roske, 2003: The Max-Planck-Institute global ocean/sea ice model with orthogonal curvilinear coordinates. *Ocean Modell.*, **5**, 91–127.
- North, G. R., R. E. Bell, and J. W. Hardin, 1993: Fluctuation dissipation in a general circulation model. *Climate Dyn.*, **8**, 259–264.
- Penland, C., 2003: A stochastic approach to nonlinear dynamics: A review. *Bull. Amer. Meteor. Soc.*, **84** (Suppl.), doi:10.1175/BAMS-84-7-Penland.
- Pohlmann, H., F. Sienz, and M. Latif, 2006: Influence of the multi-decadal Atlantic meridional overturning circulation variability on European climate. *J. Climate*, **19**, 6062–6067.
- Risken, H., 1984: *The Fokker-Planck Equation: Methods of Solution and Applications*. Springer, 454 pp.
- Roeckner, E., and Coauthors, 2003: The atmospheric general circulation model ECHAM5. Part I: Model description. Max Planck Institut for Meteorology Tech. Rep. 349, 127 pp. [Available online at http://www.mpimet.mpg.de/fileadmin/models/echam/mpl_report_349.pdf.]
- , and Coauthors, 2006: Sensitivity of simulated climate to horizontal and vertical resolution in the ECHAM5 atmosphere model. *J. Climate*, **19**, 3771–3791.
- Seiffert, R., and J.-S. von Storch, 2008: Impact of atmospheric small-scale fluctuations on climate sensitivity. *Geophys. Res. Lett.*, **35**, L10704, doi:10.1029/2008GL033483.
- Siebert, S., R. Friedrich, and J. Peinke, 1998: Analysis of data sets of stochastic systems. *Phys. Lett.*, **243A**, 275–280.
- Soden, B. J., and I. M. Held, 2006: An assessment of climate feedbacks in coupled ocean–atmosphere models. *J. Climate*, **19**, 3354–3360.
- Solomon, S., D. Qin, M. Manning, Z. Chen, M. Marquis, K. B. Averyt, M. Tignor, and H. L. Miller, Eds., 2007: *Climate Change 2007: The Physical Science Basis*. Cambridge University Press, 996 pp.
- Sura, P., 2003: Stochastic analysis of southern and Pacific Ocean sea surface winds. *J. Atmos. Sci.*, **60**, 654–666.
- , and J. Barsugli, 2002: A note on estimating drift and diffusion parameters from timeseries. *Phys. Lett.*, **305A**, 304–311.
- von Storch, J. S., 2004: On statistical dissipation in GCM climate. *Climate Dyn.*, **23**, 1–15.
- , and H. Haak, 2008: Impact of daily fluctuations on long-term predictability of the Atlantic meridional overturning circulation. *Geophys. Res. Lett.*, **35**, L01609, doi:10.1029/2007GL032385.
- Webb, M. J., and Coauthors, 2006: On the contribution of local feedback mechanisms to the range of climate sensitivity in two GCM ensembles. *Climate Dyn.*, **27**, 17–38.